Universal Fano factor and anomalous *I-V* characteristics in weakly interacting quantum dots

A. M. S. Macêdo
Departamento de Física, Laboratório de Física Teórica e Computacional, Universidade Federal de Pernambuco 50670-901 Recife, Pernambuco, Brazil

Andre M. C. Souza
Universidade Federal de Sergipe, São Cristovão-SE, Brazil
(Received 4 July 2005; published 26 October 2005)

We study interaction effects in quantum dots coupled to perfectly conducting leads via barriers of arbitrary transparencies and embedded in an electromagnetic environment characterized by a fixed external impedance. Combining a recently proposed renormalization group equation for the semiclassical regime of this system with an extended version of circuit theory, we study the Fano factor and the *I-V* characteristics in the low-temperature and low-energy regime. The Fano factor exhibits a sequence of universal plateaus as a function of the transparencies of the barriers. We also show that a recently discovered quantum transition, at intermediate values of the barrier's transparencies, leads to an anomalous transport regime characterized by a Fano factor that is the harmonic average of its values in adjacent plateaus. Our result extends a previous classification scheme for mesoscopic conductors.

DOI: 10.1103/PhysRevB.72.165340 PACS number(s): 73.23.−b, 05.45.Mt, 73.21.La

I. INTRODUCTION

The study of phase-coherent transport in open mesoscopic systems has been a fertile source of information on a variety of topics in quantum kinetics, such as measurement theory[1] and decoherence phenomena.[2] However, in spite of decades of intensive study and much progress, several fundamental issues are still not understood. The interplay between electron-electron interactions, charge discreteness, and phase-coherence in the presence of chaotic dynamics is an example of an open question in this very active research field.

From both experimental and theoretical points of view, quantum dots have proved to be excellent prototypes to address such problems. In the Coulomb blockade regime, the dot is weakly coupled to the measurement leads and electron transfer takes place via tunneling through isolated resonances, whose decay widths Γ are much smaller than k_BT. Under these conditions, the system is referred to as a "closed quantum dot" and the combination of experimental and theoretical analysis led to the development of the universal Hamiltonian concept,[3] in which the direct and the exchange interactions are modeled by constant terms, while the chaotic dynamics is described by random-matrix theory. The robustness of this scenario has recently been established by means of a renormalization group method,[4] along with the prediction of an interesting phase with a spontaneous Fermi surface distortion.[5]

Increasing the coupling between the system and its environment induces quantum charge fluctuations, which smears the Coulomb gap in the *I-V* characteristics and adds new time scales to the problem, making it much more challenging. In fact, the formulation of a consistent many-body problem under such conditions, where the system is referred to as an "open quantum dot," is a very nontrivial task, as can be seen from the history of the field, which has not been without conflicting results from different models. Presently, there are two main, well-developed approaches to this problem and their results are now begining to be reconciled in a single unified scheme.[6–8] The first one[6] is a clever combination of the real-time path integral formalism with the random scattering matrix approach to quantum transport. It is based on the use of the Feynman-Vernon[9] formalism of dissipative quantum mechanics to derive a nonlinear effective field theory describing voltage fluctuations in a macroscopic electric circuit in which a coherent scatterer exhibiting electron-electron interactions and chaotic dynamics is embedded. It is also known as the environmental formalism and its technique turned out to be very flexible, yielding a great variety of results, both perturbative and nonperturbative. The second approach is based on a bosonization scheme that exploits the one-dimensionality of the point contacts between the dot and its environment. It has had much success in describing the incoherent regime, but has led to incorrect predictions for the coherent case (for a detailed historical account, see Ref. 8). However, in a recent development of this formalism,[7,8] a trick based on the inclusion of a fictitious lead at the point of contact is employed to set up a calculational scheme for performing a perturbative expansion around the semiclassical limit of a large number of scattering channels in the contacts. The results coincide with those of the environmental formalism and provide an important unification of the theoretical models for open quantum dots.

A common feature of the calculational schemes described above is the fact that they both correspond to an "external approach," in the sense discussed in Ref. 10. The degrees of freedom associated with the dynamics inside the quantum dot are eliminated in favor of those inside the leads or in the electromagnetic environment. As a consequence, the final, sample specific expressions can be written in terms of a random scattering matrix describing the dynamics of a noninteracting chaotic dot. Ensemble average is then performed using directly the distribution function of the scattering matrix. As pointed out in Ref. 10, we may just as well eliminate all

degrees of freedom outside the dot and thus construct an "internal approach." One of the advantages of this alternative route is the possibility of performing the ensemble average at an early stage, thereby deriving an effective nonlinear σ model, thus making the theory fully nonperturbative. The central motivation to incorporate many-body effects in a mesoscopic transport formalism in such a way is to find the correct extension, incorporating electron-electron interactions, of the very successful supersymmetric nonlinear σ-model description of noninteracting mesoscopic systems.[11] To be more specific, one aims at building an effective field theory to describe, on equal footing, quantum interference, chaotic dynamics, and interaction effects at arbitrary values of the system-lead coupling. The complexity of this general problem stems from the large number of competing time scales, which usually leads to highly nonlinear effective field theories with long memory effects and possibly making nonperturbative calculations nearly intractable. Important recent efforts in this direction have been made in Ref. 12, where a low-energy effective σ model was constructed using the Keldysh formalism to describe disordered interacting metals in terms of quantum fluctuations of the electron distribution function. The model contains two independent fluctuating fields and a very complicated action, but its saddle-point equation turned out to lead to an insightful quantum kinetic equation with several interesting applications.[12,13] The recent direct measurement[14] of the nonequilibrium energy distribution function of quasiparticles in a diffusive mesoscopic wire makes such an approach particularly appealing.

In Ref. 10 an alternative external approach was presented in which the separation of time scales is dealt with by using the projection, or memory function, technique.[15] The main ingredient in this formalism is the many-body quantum-mechanical treatment of the whole system: sample, leads, and detectors. The entire mathematical structure is built from a specific measurement procedure, viz. the charge counting statistics. Using the geometric formulation[16] of the memory-function formalism, it was possible to project the dynamics of the whole system onto the single particle subspace, which allowed the emergence of the Keldysh single particle Green's function with a very general double time self-energy function. Elimination of the degrees of freedom inside the leads yielded a many-body generalization of the Levitov-Lesovik functional determinant formula, i.e., the generating function of the charge counting statistics. The main attractive technical features of this formalism are (i) a suitable mathematical structure in which to implement controlled and conserving approximations, (ii) no need to introduce unphysical local chemical potentials throughout the system and (iii) a natural connection with powerful field theoretical methods, such as the supersymmetry technique[11] and Keldysh nonlinear σ models[12] along with several renormalization schemes.[17] From the viewpoint of the memory function formalism, the crux of the matter is the appropriate selection of the set of relevant variables. Conserved quantities and pointer states of measurement devices are natural candidates, but there may be hidden degrees of freedom with large time scales that could exchange information with the selected set during the dynamical evolution and, therefore, should also be retained as relevant. As pointed out in Ref. 16, the correct identification of the relevant set is both crucial, for justifying approximations, and difficult to implement since there is no systematic prescription. The safest procedure seems to be to stay as close as possible to successful dynamical models covering well-known nearby regimes, where wide separation of time scales may prevent the appearance of large memory effects due to some overlooked degrees of freedom, which could become relevant when the system is perturbed by the inclusion of new dynamical ingredients, such as interaction and/or disorder. In the problem of an open chaotic quantum dot in the presence of Coulomb interactions, the zero-dimensional supersymmetric nonlinear σ model, which describes exactly the ergodic regime of the noninteracting limit, appears to be the best candidate for such a starting point, as has been confirmed by the S-matrix expansion obtained from both the environmental path-integral formalism[6] and the bosonization approach.[7,8]

An important general scheme to derive realistic effective models consists of using renormalization group (RG) transformations to eliminate the irrelevant degrees of freedom and to absorb memory effects in a renormalization of bare parameters in the minimal description of the dynamics of the relevant observables (the unperturbed action in the functional integral approach). Indeed quite recently, Kindermann and Nazarov[18] studied the main effect of weak elastic electron-electron interactions in an open mesoscopic conductor using an electromagnetic environment model together with a renormalization group scheme similar to that of Ref. 19. They argued that at low-energy scales, macroscopic degrees of freedom associated with the electromagnetic environment can account for the dominant features of Coulomb interactions inside the conductor. The impedance $Z(\omega)$ of the external circuit at a characteristic frequency scale Ω, set, e.g., by the voltage V at the conductor, becomes a measure of the interaction strength and might lead to a dynamical Coulomb blockade.[20] For weak interactions, however, the main effect is the emergence of an anomalous low-bias I-V characteristics, $I(V) \propto V^{2z+1}$, where $z \equiv e^2 Z(\Omega)/h \ll 1$. Using perturbation theory in z and a renormalization group argument, the authors of Ref. 18 showed that in the case of weak interactions, the leading contributions can be incorporated in an appropriate energy dependence of transmission eigenvalues of the corresponding noninteracting system. From the RG flow equations, the authors concluded that there were only two possible universal low-energy scenarios. In the first one, the main effect of weak Coulomb interactions is to suppress electron transport by shifting the transmission eigenvalue distribution toward zero and making the conductor behave as a single tunnel junction. The second possibility appears when there exists an inverse square-root singularity in the average transmission eigenvalue density at unit transmission yielding a limiting distribution function similar to that of a symmetric double junction. The general consequence of this conclusion is the prediction of only two exponents for the asymptotic power-law behavior of the low-energy and low-temperature differential conductance of weakly interacting quantum dots.

Motivated by these results, we address in this paper the following questions: (i) What features of the effective field theory describing open interacting quantum dots in the context of the memory-function formalism of Ref. 10 can be

extracted from the renormalization group flow equations of Ref. 18; (ii) Are the predictions of Ref. 18 of only two universality classes for mesoscopic conductors really exhaustive in the light of recent developments, applying an extended version of circuit theory,[21–23] in the quantitative description of the average density of transmission eigenvalues of noninteracting open quantum dots? As we shall demonstrate in this work, both questions yield interesting answers. First, we show that in the semiclassical regime, it is possible to absorb all effects of weak elastic Coulomb interactions in an effective gauge potential coupled to the matrix field of the supersymmetric nonlinear σ model. Second, we found a different universality class for the low-energy, low-temperature sector of the theory, associated with a recently reported quantum transition related to the emergence of Fabry-Perot modes between the barriers, which are responsible for an inverse square-root singularity in the average transmission eigenvalue density at unit transmission.

This paper is organized as follows. In Sec. II, we present a constructive version of the many-body formula for full counting statistics presented in Ref. 10. A random matrix model and its associated supersymmetric nonlinear σ model representation are introduced to describe the noninteracting limit of a quantum dot coupled to the environment via two barriers of arbitrary transparencies. In Sec. III, we discuss in detail the relevant time scales of the problem and present the renormalization group flow equation that connects the noninteracting limit to the weak interacting regime. In Sec. IV, we review the extended version of circuit theory that captures the information content in the saddle point of the nonlinear σ model, and we summarize the main results of a recently reported continuous quantum transition related to the formation of Fabry-Perot resonances between the semitransparent barriers. The low-energy power-law behavior of the differential conductance is analyzed in detail in Sec. V for systems with various barrier configurations (symmetric, tunnel, and general). In Sec. VI, an experimental procedure is proposed to measure the anomalous exponent of the differential conductance by means of the Fano factor (the ratio between the shot noise power and the conductance), which exhibits universal plateaus in the low-energy regime. A summary and conclusions are presented in Sec. VII.

II. THE MODEL SYSTEM

In this section, we introduce the basic model system, which we shall use to interpret the results presented in this paper. It consists of a combination of the memory-function formalism of Ref. 10 with random-matrix theory and the supersymmetric nonlinear σ model. We start by deriving a simplified, ready to use, version of the general many-body formula for full counting statistics (FCS) presented in Ref. 10.

A. A many-body formula for full counting statistics

We consider an isolated quantum dot with an arbitrary number of particles, whose dynamics is described by the following general many-body Hamiltonian

$$H = \int_{\Omega} d\mathbf{r}\,\psi^{\dagger}(\mathbf{r})\left(\frac{p^2}{2m} + U(\mathbf{r})\right)\psi(\mathbf{r}) + \int_{\Omega} d\mathbf{r} \int_{\Omega} d\mathbf{r}'\, u(\mathbf{r},\mathbf{r}')\psi^{\dagger}(\mathbf{r})\psi^{\dagger}(\mathbf{r}')\psi(\mathbf{r}')\psi(\mathbf{r}),$$

where Ω is the configuration space of the dot, $\psi(\mathbf{r})$ is the electron field operator, $U(\mathbf{r})$ is a single-particle potential, and $u(\mathbf{r},\mathbf{r}')$ is an arbitrary many-body potential. Using the Keldysh formalism, we may describe the dynamics inside the dot by means of three, real-time, one-particle Green's functions, viz. the retarded and advanced propagators, given respectively by

$$g^{r}(x,x') = -i\theta(t-t')\langle\{\psi(x),\psi^{\dagger}(x')\}\rangle, \tag{1}$$

and

$$g^{a}(x,x') = i\theta(t'-t)\langle\{\psi(x),\psi^{\dagger}(x')\}\rangle, \tag{2}$$

where $x=(\mathbf{r},t/\hbar)$, and the Keldysh function

$$g^{K}(x,x') = -i\langle[\psi(x),\psi^{\dagger}(x')]\rangle. \tag{3}$$

In the above expressions, $\{A,B\}=AB+BA$ and $[A,B]=AB-BA$ are the anticomutator and comutator, respectively. For technical convenience, these Green's functions are usually accommodated into a single matrix function defined as

$$\bar{g} = \begin{pmatrix} g^{r} & g^{K} \\ 0 & g^{a} \end{pmatrix}, \tag{4}$$

and, as usual, we shall adopt the following product convention:

$$(\bar{A}\bar{B})(x,x') = \int dx''\bar{A}(x,x'')\bar{B}(x'',x'), \tag{5}$$

where $dx=d\mathbf{r}dt/\hbar$.

Following Ref. 10, we assume an adiabatic coupling of the dot to an electromagnetic environment, containing two leads connected to a generator supplying an electromotive force and a charge detector with a counting field, $\lambda(t)$, located at one of the lead-dot interfaces. The environmental degrees of freedom can be eliminated using the projection formalism, and we end up with a Dyson equation for a renormalized single-particle matrix Green's function. In the absence of the counting field, it reads simply

$$\bar{G} = \bar{g} + \bar{g}\bar{\Sigma}\bar{G} = \bar{g} + \bar{G}\bar{\Sigma}\bar{g}, \tag{6}$$

where $\bar{\Sigma}(x,x')$ is the memory function associated with the residual effects, in the dot dynamics, of the eliminated degrees of freedom. The presence of the counting field at the lead-dot interface is incorporated in the formalism via the following gauge transformation:

$$\bar{A}^{\lambda}(x,x') = e^{i\bar{a}_{\lambda}(x)}\bar{A}(x,x')e^{-i\bar{a}_{\lambda}(x)}, \tag{7}$$

where

$$\bar{a}_\lambda(x) = \frac{1}{2}\bar{\sigma}\lambda(t)\theta[F(\mathbf{r})], \tag{8}$$

with the equation, $F(\mathbf{r})=0$, specifying the lead-dot interface at which an ideal charge detector is placed. The matrix

$$\bar{\sigma} = \begin{pmatrix} 0 & 1 \\ 1 & 0 \end{pmatrix} \tag{9}$$

is a Pauli matrix and the counting field has the form

$$\lambda(t) = \theta(t)\,\theta(T_0 - t)\lambda + \delta\lambda(t), \tag{10}$$

in which $\delta\lambda(t)$ is a function that interpolates smoothly between $-\lambda$ and zero outside the measurement interval $0 \leqslant t \leqslant T_0$. The total charge transmitted through the dot during observation time T_0 is then given by

$$Q = -ie\ \frac{\partial}{\partial\lambda}\Phi(\lambda)\bigg|_{\lambda=0}, \tag{11}$$

where

$$\Phi(\lambda) = \mathrm{Tr}\ \ln[1 + \bar{G}^\lambda(\bar{\Sigma}^\lambda - \bar{\Sigma})] \tag{12}$$

is the generating function of the full counting statistics of the interacting dot coupled to an electromagnetic environment. The gauge transformed Green's function $\bar{G}^\lambda$ satisfies the Dyson equation

$$\bar{G}^\lambda = \bar{g} + \bar{g}\bar{\Sigma}^\lambda\bar{G}^\lambda = \bar{g} + \bar{G}^\lambda\bar{\Sigma}^\lambda\bar{g}. \tag{13}$$

The self-energy $\bar{\Sigma}^\lambda$ can be decomposed, assuming absence of direct processes between different leads, in terms of functions localized at the interfaces (labeled 1 and 2) as follows:

$$\bar{\Sigma}^\lambda = e^{i\lambda\bar{\sigma}/2}\bar{\Sigma}_1 e^{-i\lambda\bar{\sigma}/2} + \bar{\Sigma}_2. \tag{14}$$

Combining Eqs. (6) and (13), we obtain the following equations:

$$\bar{G}^\lambda = \bar{G} + \bar{G}(\bar{\Sigma}^\lambda - \bar{\Sigma})\bar{G}^\lambda = \bar{G} + \bar{G}^\lambda(\bar{\Sigma}^\lambda - \bar{\Sigma})\bar{G},$$

from which we deduce the formula

$$\chi(\lambda) \equiv e^{-\Phi(\lambda)} = \det\left(\frac{\bar{G}}{\bar{G}^\lambda}\right). \tag{15}$$

Using this equation, we may formally compute the probability P_n that a number n of particles is transmitted through the interface during time T_0, via the relation

$$P_n = \int_{-\pi}^{\pi}\frac{d\lambda}{2\pi}\chi(\lambda)e^{-in\lambda}. \tag{16}$$

We may further simplify the model by exploiting the natural separation of time scales in the problem. This can be achieved by imposing a simplified form for the memory matrix, which is generally defined as

$$\bar{\Sigma}_p(x,x') \equiv \begin{pmatrix} \Sigma_p^r(x,x') & \Sigma_p^K(x,x') \\ 0 & \Sigma_p^a(x,x') \end{pmatrix}. \tag{17}$$

For the Keldysh component, we set

$$\Sigma_p^K(x,x') = i\Gamma_p(\mathbf{r},\mathbf{r}')[2n(\tau)e^{-i\Delta_p(\tau)} - \hbar\,\delta(\tau)], \tag{18}$$

where $\tau \equiv t - t'$ and $\Gamma_p(\mathbf{r},\mathbf{r}')$ is an energy-independent linewidth function associated with the tunneling rates between lead p and the dot. The time-dependent phase shift

$$\Delta_p(\tau) = -\frac{e\tau}{\hbar}V_p, \tag{19}$$

describes the effect of a local self-consistent electrostatic potential V_p. The occupation function $n(\tau)$ is pinned at the interface in a quasiequilibrium value

$$n(\tau) = \int_{-\infty}^{\infty}\frac{dE}{2\pi}f(E)e^{-iE\tau/\hbar}, \tag{20}$$

where $f(E)$ is the reduced single-particle distribution function. Finally, the retarded and advanced components are given by

$$\Sigma_p^{r,a}(x,x') = \mp\frac{i}{2}\Gamma_p(\mathbf{r},\mathbf{r}')\hbar\,\delta(\tau). \tag{21}$$

Performing the Fourier transform, we obtain

$$\Sigma_p^K(\mathbf{r},\mathbf{r}';E) = i\Gamma_p(\mathbf{r},\mathbf{r}')[2f_p(E) - 1], \tag{22}$$

for the Keldysh component, where $f_p(E) = f(E + eV_p)$, and

$$\Sigma_p^{r,a}(\mathbf{r},\mathbf{r}';E) = \mp\frac{i}{2}\Gamma_p(\mathbf{r},\mathbf{r}') \tag{23}$$

for the retarded and advanced components.

Using the above expressions and performing the trace over the Keldysh 2×2 matrix space, we can rewrite Eq. (12) in the following much simpler and useful form:

$$\Phi(\lambda) = -\frac{T_0}{h}\int_{-\infty}^{\infty}dE\ \mathrm{Tr}\ \ln[1 + J_\lambda(E)A(E)], \tag{24}$$

in which, we introduced the scalar function

$$J_\lambda(E) = (e^{i\lambda} - 1)f_1(E)[1 - f_2(E)] + (e^{-i\lambda} - 1)f_2(E)[1 - f_1(E)] \tag{25}$$

and the "continuous matrix" $[A(E)](\mathbf{r},\mathbf{r}') \equiv A(\mathbf{r},\mathbf{r}';E)$, where

$$A(E) = \Gamma_1 G^r(E)\Gamma_2 G^a(E). \tag{26}$$

Equation (24) is the central result of this section. It complements the results of Ref. 10 and corresponds to a constructive many-body generalization of Levitov's FCS formula. Note that $G^{r,a}(\mathbf{r},\mathbf{r}';E)$ are full many-body Green's functions containing, in principle, all interaction effects inside the dots. Just like Levitov's formula, Eq. (24) is sample specific, which in the presence of chaotic dynamics signifies that it fluctuates strongly in the energy domain on scales of the order of the dot's mean level spacing. We may smooth out these fluctuations and recover universal properties by performing an ensemble average over identically prepared systems, or by integrating over a sufficiently large energy window. Either way, such averaging procedure amounts to a replacement of the fast electron propagator by much slower

density relaxation modes, usually coupled to external sources and amenable to a description in terms of a nonlinear σ model.

The main difficulty with this direct approach is the complexity of the resulting effective action, which is both nonlinear in the fields and nonlocal in time. In this work, we shall adopt an alternative route that is more efficient to account for weak interactions in the presence of an electromagnetic environment. We start by employing the renormalization group flow equation, derived in Ref. 18, and at a later stage, in the calculation of observables, we shall interpret the formulas in terms of an underlying effective nonlinear σ model. With this in mind, we discuss, in Sec. II C, the noninteracting limit of Eq. (24) and introduce a stochastic model based on random-matrix theory for performing the ensemble average, which directly yields the associated supersymmetric nonlinear σ model.

B. Random-matrix model for open chaotic cavities

The dynamics of a noninteracting particle in a chaotic quantum dot can be efficiently described by a stochastic model introduced by Verbaarschot, Weidenmüller, and Zirnbauer (VWZ).[24] It amounts to specifying the linewidth matrix in terms of rectangular coupling matrices W_p, so that

$$\Gamma_p = 2\pi W_p W_p^\dagger, \quad p = 1,2. \tag{27}$$

In addition, one assumes the orthogonality condition

$$(W_p^\dagger W_q)_{nm} = \frac{\gamma}{\pi}\delta_{pq}\delta_{nm}w_{pn}, \tag{28}$$

where $w_{pn} \geqslant 0$ quantifies the dot-lead coupling strength. The parameter γ fixes the mean level spacing, $\Delta = \pi\gamma/M$, of the M resonances in the dot, close to the center of the spectrum ($E=0$). The retarded and advanced Green's functions are given by

$$G^{r,a}(E) = [E - H \pm (i/2)(\Gamma_1 + \Gamma_2)]^{-1}, \tag{29}$$

where H is an $M \times M$ random Hamiltonian matrix taken from the Gaussian unitary ensemble (GUE), which is appropriate for systems with broken time-reversal symmetry, so that

$$\langle H_{\mu\nu}\rangle = 0 \tag{30}$$

and

$$\langle H_{\mu\nu}H_{\mu'\nu'}\rangle = \frac{\gamma^2}{M}\delta_{\mu\nu'}\delta_{\nu\mu'}. \tag{31}$$

The scattering matrix at $E=0$ reads

$$S_{nm}^{pq} = \delta_{pq}\delta_{nm} - 2\pi i \sum_{\mu\nu} (W_p^\dagger)_{n\mu}(G^r)_{\mu\nu}(W_q)_{\nu m}, \tag{32}$$

which allows the definition of the transmission coefficients of the barriers at the lead-dot interfaces

$$T_{pn} = 1 - |\langle S_{nm}^{pq}\rangle|^2. \tag{33}$$

From the above definitions, one obtains

$$\langle S_{nm}^{pq}\rangle = \delta_{pq}\delta_{nm}\tanh(\alpha_{pn}/2), \tag{34}$$

where $\alpha_{pn} = -\ln w_{pn}$. Inserting Eqs. (34) into (33) yields

$$T_{pn} = \mathrm{sech}^2(\alpha_{pn}/2). \tag{35}$$

In this model, the transmission matrix, $t(E)$, is given by

$$t(E) = -2\pi i W_1^\dagger G^r(E) W_2. \tag{36}$$

Using this result and taking the zero temperature limit, Eq. (24) becomes the Levitov formula of FCS[25]

$$\Phi(\lambda) = -M_0 \,\mathrm{Tr}\ln[1 + (e^{i\lambda} - 1)tt^\dagger], \tag{37}$$

where $M_0 = eVT_0/h$ is the number of attempts to transmit an electron during the observation time T_0 and the Fermi energy is placed at the band center ($E_F = 0$). The irreducible cumulants of FCS are defined via the series expansion

$$\Phi(\lambda) = -\sum_{k=1}^{\infty} \frac{(i\lambda)^k}{k!} q_k, \tag{38}$$

where

$$q_k =: -\frac{d^k}{d(i\lambda)^k}\Phi(\lambda)\bigg|_{\lambda=0}. \tag{39}$$

Some examples are the Landauer conductance formula

$$g = q_1/M_0 = \mathrm{Tr}(tt^\dagger) \tag{40}$$

and the shot-noise power

$$p = q_2/M_0 = \mathrm{Tr}[tt^\dagger(1 - tt^\dagger)]. \tag{41}$$

C. The supersymmetric nonlinear σ model

One of the main advantages of the above random-matrix model is the ease with which ensemble averages can be mapped onto integrals over coset spaces of supersymmetric nonlinear σ models. To illustrate this point, define the arbitrary complex vectors $\mathbf{a} = (a_1, a_2), \mathbf{b} = (b_1, b_2)$, and consider the following generating function:[26]

$$Z(\mathbf{a},\mathbf{b}) = \det\left(\frac{1 - b_1 b_2 tt^\dagger}{1 - a_1 a_2 tt^\dagger}\right), \tag{42}$$

where t is the random transmission matrix defined in Eq. (36) at $E=0$. Let $\Psi(\mathbf{a},\mathbf{b})$ be the ensemble average of $Z(\mathbf{a},\mathbf{b})$, then, for systems with unitary symmetry, one can show that

$$\Psi(\mathbf{a},\mathbf{b}) = \int_{Q^2=1} dQ f_1(Q_{\mathbf{ab}}, Q) f_2(Q, Q_0), \tag{43}$$

in which

$$f_p(Q,Q') = \prod_{n=1}^{N_p} \mathrm{Sdet}^{-1/2}(1 + e^{-\alpha_{pn}}QQ'), \quad p = 1,2 \tag{44}$$

are coupling functions describing the lead-dot interfaces. The barriers' transparencies appear through the variables α_{pn} related to the transmission coefficients T_{pn}, via Eq. (35). We adopt the standard notation for operations in supermathemat-

ics: Sdet stands for the superdeterminant and dQ is the invariant measure of Efetov's coset space. A useful parametrization of Q is[11]

$$Q = U\begin{pmatrix} \cos\hat{\theta} & i\sin\hat{\theta} \\ -i\sin\hat{\theta} & -\cos\hat{\theta} \end{pmatrix}U^{-1}, \tag{45}$$

where $\hat{\theta} \equiv \mathrm{diag}(i\theta_1, i\theta_1, \theta_0, \theta_0)$, $\theta_1 > 0$, $0 < \theta_0 < \pi$, and U is a pseudounitary supermatrix. The special point, $Q_0 = \mathrm{diag}(1,1,1,1,-1,-1,-1,-1)$, represents the origin of the coset space. The external parameters appear in the source matrix, $Q_{\mathbf{ab}} \equiv SQ_0S^{-1}$, where

$$S = \exp\begin{pmatrix} 0 & iX_1 \\ iY_1 & 0 \end{pmatrix}\exp\begin{pmatrix} 0 & iY_2 \\ iX_2 & 0 \end{pmatrix}, \tag{46}$$

with $X_j = \mathrm{diag}(a_j, 0, b_j, 0)$ and $Y_j = \mathrm{diag}(0, a_j, 0, b_j)$.

The average of the generating function of FCS can be calculated from $\Psi(\mathbf{a},\mathbf{b})$ as follows. Define the auxiliary function

$$q(\lambda) \equiv i\frac{\partial\langle\Phi(\lambda)\rangle}{\partial\lambda} = M_0\,\mathrm{Tr}\left\langle \frac{e^{i\lambda}tt^{\dagger}}{1+(e^{i\lambda}-1)tt^{\dagger}} \right\rangle, \tag{47}$$

then, from Eq. (42) we can see that

$$q(\lambda) = M_0\frac{\partial\Psi(\mathbf{a},\mathbf{b})}{\partial a_2}\bigg|_{\mathbf{a}=(e^{i\lambda},e^{-i\lambda}-1)=\mathbf{b}}. \tag{48}$$

This formula will be used later to calculate the average semiclassical conductance of a weakly interacting open quantum dot. With this in mind, we shall, in Sec. III, discuss the relevant time scales in the problem and some immediate consequences of the renormalization group flow equation proposed by Kindermann and Nazarov.[18]

III. TIME SCALES AND RG FLOW EQUATION

As we pointed out in Sec. II, the connection between the full interacting formula for counting statistics, Eq. (24), and the generating function of the nonlinear σ model, Eq. (43), is not a direct one (except in the case where interactions can be neglected). However, one cannot rule out the possibility that, by proper separation of some relevant time scales, one could produce a renormalization group argument in which the noninteracting limit evolves into the interacting one via a scaling or flow equation. The analytical solution of such an equation might be interpreted as resulting from an effective nonlinear σ model for the corresponding physical regime. This is precisely what we are going to do in this section. We start by discussing, in Sec. III A, the relevant time scales in the problem.

A. Time scales

Since we shall be concerned with universal properties, we require that the ergodic time, $t_{erg} \simeq L/v_F$, where L is the linear dimension of the dot and v_F is the Fermi velocity, be the smallest time scale in the problem. Another important scale is the Heisenberg time, $t_H \simeq \hbar/\Delta$, where $\Delta = \pi\gamma/M$ is the mean level spacing in the dot. It sets the scale at which the discrete structure of the spectrum affects the dynamics in the dot. If a resonance is formed inside the dot, its lifetime is roughly the inverse of the correlation width, $\Gamma_{corr} = [\Delta/(2\pi)]\Sigma_{np}T_{pn}$, for fluctuations of S-matrix elements at different energies. We may thus define the dwell time, $t_D \simeq \hbar/\Gamma_{corr}$, and in this way we obtain the Thouless energy of the open dot, $E_T = \hbar/t_D$. An important parameter in the theory is the Thouless conductance, defined as $g_T \equiv E_T/\Delta \simeq t_H/t_D$, which can be used to define the semiclassical regime by the condition $g_T \gg 1$. Charge relaxation in the dot is controlled by the RC time, $t_{rel} = R_TC$, where $R_T = h/(e^2g_T)$ is the charge-relaxation resistance[27] and C is the effective capacitance of the dot. The charge discreteness correlation time describes the fast fluctuations in the current on the time scale of the transmission attempts, $t_\Omega \simeq \hbar/\Omega$, where $\Omega \equiv \max(eV, k_BT)$, in which V is the applied voltage and T is the system's temperature. We are now in a position to define the physical regime, which we shall be concerned with, in terms of large separations of the above time scales: $t_{erg} \ll t_{rel} \ll t_\Omega \ll t_D$.

B. Renormalization group flow equation

If Coulomb interaction inside the dot is weak, charging effects may be washed out by quantum charge fluctuations. The interaction strength can be measured via the impedance, $Z(\Omega)$, of the electromagnetic environment in which the system is embedded.[28] Dynamic Coulomb blockade is strongly suppressed if $z = (e^2/h)Z(\Omega) \ll 1$. In tunnel junctions,[20] this suppression can be understood as the analogous of the Mössbauer effect, in which recoilless γ emission takes place whenever the change in the momentum of the nucleus is much smaller than its spontaneous zero-point fluctuations. In the electronic problem, elastic (dissipationless) tunneling events dominate when the change in the effective charge of the capacitor is much smaller than the spontaneous quantum fluctuations of the electric charge. This effect can be measured via the I-V characteristics, which exhibit a zero-bias anomaly with a power-law behavior $I(V) \simeq V^{2z+1}$. This same power law was found for tunnel contacts between Luttinger liquid,[29] and contacts with arbitrary transmission for weakly interacting single-channel conductors.[19] In Ref. 18, this latter result was extended for conductors with an arbitrary number of channels. The renormalization group procedure used by these authors is a multichannel generalization of that of Ref. 19. It amounts to selecting an energy window of relevant states (of the order of the inverse RC time of the conductor) and mapping the problem onto a similar one with energy-dependent renormalized transmission eigenvalues, which accounts for effective couplings with excluded states. The renormalization group transformations can be interpreted in terms of changes in the average transmission eigenvalue density of a generic mesoscopic conductor caused by an energy dependence of transmission eigenvalues. The flow equation reads

$$\frac{d\tau_n(E)}{d\ln E} = 2z\tau_n(1-\tau_n). \tag{49}$$

A similar RG equation was recently derived in Ref. 6 directly from a semiclassical expansion (see also Ref. 30). Equation (49) can be integrated to yield

$$\tau_n(\varepsilon) = \frac{\varepsilon^2 \tau_n}{1 + (\varepsilon^2 - 1)\tau_n}, \tag{50}$$

in which $\varepsilon \equiv (E/E_{rel})^z$ and $E_{rel} = \hbar/t_{rel} = g_T E_C$ is the inverse charge-relaxation time of the conductor and $E_C = e^2/C$ is the charging energy. It is assumed that at $\varepsilon = 1$, the transmission eigenvalues reach the energy-independent values of the corresponding noninteracting system. The conductance of the system is given by the renormalized Landauer formula

$$g(\varepsilon) = \sum_{n=1}^{N} \tau_n(\varepsilon) = \mathrm{Tr}\left(\frac{\varepsilon^2 tt^\dagger}{1 + (\varepsilon^2 - 1)tt^\dagger} \right), \tag{51}$$

whose average value can be obtained directly from the semiclassical limit of the σ model

$$\langle g(\varepsilon) \rangle = \varepsilon^2 \frac{\partial \Psi_{sc}(\mathbf{a},\mathbf{b})}{\partial a_2}\bigg|_{\mathbf{a}=(\varepsilon^2, \varepsilon^{-2}-1)=\mathbf{b}}, \tag{52}$$

where the subscript *sc* stands for semiclassical. The generating function of FCS can also be written in terms of the renormalized transmission coefficients, $\tau_n(\varepsilon)$. It reads

$$\Phi(\lambda, \varepsilon) = -M_0 \sum_{n=1}^{N} \ln\left(1 + (e^{i\lambda} - 1)\tau_n(\varepsilon)\right) \tag{53}$$

and, therefore,

$$q(\lambda, \varepsilon) \equiv i \frac{\partial \langle \Phi(\lambda, \varepsilon) \rangle}{\partial \lambda} = M_0 \, \mathrm{Tr} \left\langle \frac{\varepsilon^2 e^{i\lambda} tt^\dagger}{1 + (\varepsilon^2 e^{i\lambda} - 1)tt^\dagger} \right\rangle. \tag{54}$$

We can also calculate this quantity directly from the semiclassical limit of the average generating function of the σ model, $\Psi_{sc}(\mathbf{a},\mathbf{b})$, using the formula

$$q(\lambda, \varepsilon) = M_0 \frac{\partial \Psi_{sc}(\mathbf{a},\mathbf{b})}{\partial a_2}\bigg|_{\mathbf{a}=(\varepsilon^2 e^{i\lambda}, \varepsilon^{-2} e^{-i\lambda} - 1)=\mathbf{b}}. \tag{55}$$

Equations (52) and (55) are the central results of this section. They establish an interesting extension in the domain of validity of the semiclassical limit of the nonlinear σ model by incorporating the regime of weak Coulomb interactions via the presence of an external energy-dependent supermatrix gauge field: $Q_{\mathbf{ab}}(\varepsilon)$.

IV. THE SEMICLASSICAL LIMIT OF THE σ MODEL

Up to this point, we have managed to relate all quantities of interest to the semiclassical limit of the average generating function, $\Psi_{sc}(\mathbf{a},\mathbf{b})$. The predictive power of the formalism, therefore, hinges upon our ability to calculate this function. In Refs. 21 and 23, it was shown that in this semiclassical limit, defined by requiring the number of open scattering channels to be large, i.e., $N_1, N_2 \gg 1$, the information contained in the saddle-point equations of the σ model can be cast in the form of an extension of Nazarov's circuit theory. In Sec. IV A, we briefly review the principal features of this approach.

A. Circuit theory for the σ model

The extended form of circuit theory can be formulated in terms of a pseudocurrent, defined from the σ model as

$$K(x) \equiv \frac{\partial \Psi_{sc}(\mathbf{a},\mathbf{b})}{\partial a_2}\bigg|_{\mathbf{a}=(\sinh x \cosh x, -\tanh x)=\mathbf{b}}, \tag{56}$$

which can also be written as

$$K(x) = \frac{1}{2} \mathrm{Tr} \left\langle \frac{\sinh(2x) tt^\dagger}{1 + \sinh^2(x) tt^\dagger} \right\rangle. \tag{57}$$

The variable x plays the role of a pseudopotential, so that $K(x)$ is similar to the current-voltage characteristic of a circuit element. Let $K_p(\Delta x)$, $p = 1, 2$, denote the pseudocurrent through barrier p (interpreted as a circuit element), where Δx is the pseudopotential drop, then using Eq. (43) one can show that[21]

$$K_p(\Delta x) = \sum_{n=1}^{N_p} \frac{\sinh(2\Delta x)}{\cosh(2\Delta x) + \cosh \alpha_{pn}}. \tag{58}$$

For a double barrier chaotic quantum dot, Eq. (58) should be used together with the following pseudocurrent conservation law

$$K(x) = K_1(x - y) = K_2(y). \tag{59}$$

Here, we shall be concerned with the particular case of asymmetric barriers with N equivalent channels, for which Eq. (58) simplifies to

$$K_p(x) = \frac{N}{2}\left[\tanh\left(x + \frac{1}{2}\alpha_p \right) + \tanh\left(x - \frac{1}{2}\alpha_p \right) \right]. \tag{60}$$

The constants α_p are related to the barriers' transparencies via the relation $T_p = \mathrm{sech}^2(\alpha_p/2)$. Inserting Eq. (60) into Eq. (59) yields

$$\tanh\left(x - y + \frac{1}{2}\alpha_1 \right) + \tanh\left(x - y - \frac{1}{2}\alpha_1 \right) = \tanh\left(y + \frac{1}{2}\alpha_2 \right) + \tanh\left(y - \frac{1}{2}\alpha_2 \right). \tag{61}$$

Using the trigonometric identity

$$\tanh(x - y) = \frac{\tanh x - \tanh y}{1 - \tanh x \tanh y}, \tag{62}$$

we obtain the following fourth-degree equation for the variable $\xi = \tanh y$

$$\begin{aligned} &[T_1(1 - T_2)\tanh x]\xi^4 - (3T_1 T_2 \tanh x)\xi^2 \\ &\quad + [(T_1 T_2 + T_2 - T_1)\tanh^2 x + 2T_1 T_2 - T_1 - T_2]\xi^3 \\ &\quad + [(T_1 T_2 + T_1 - T_2)\tanh^2 x + T_1 + T_2]\xi - T_1 \tanh x = 0. \end{aligned} \tag{63}$$

From the physical root of Eq. (63) we may calculate the pseudocurrent through the relation

$$K(x) = \frac{NT_2\xi}{1-(1-T_2)\xi^2}. \tag{64}$$

Equations (63) and (64) are the circuit theory equations for the double barrier chaotic quantum dot. In Ref. 22, these equations were shown to be equivalent to a set of coupled nonlinear equations derived, for the same system, from the diagrammatic method for integration over the unitary group, developed by Brouwer and Beenakker.[31] Solutions of Eqs. (63) and (64) for several particular cases, such as symmetric barriers ($T_1=T=T_2$) and tunnel junctions ($T_1, T_2 \ll 1$) were presented in Ref. 23. In Sec. IV B, we shall briefly discuss the quantum transition studied in detail in Ref. 23, which is due to the formation of Fabry-Perot resonances between the barriers and which will play a decisive role in the behavior of $\langle g(\varepsilon)\rangle$ for $\varepsilon \ll 1$.

B. Formation of Fabry-Perot resonances

The importance of Fabry-Perot (FP) resonances to the behavior of the low-voltage, low-temperature differential conductance of weakly interacting quantum dots was already pointed out by Kindermann and Nazarov in their analysis of the renormalization group flow equation, Eq. (49). They did not, however, consider the possibility of a continuous quantum transition in which the density of FP resonances may act as a kind of order parameter. The existence of such a transition and its characterization was the central result of Ref. 23.

The emergence of an inverse square-root singularity at unit transmission, i.e., $\tau=1$, in the transmission eigenvalue density, defined as $\rho(\tau)=\mathrm{Tr}\langle\delta(\tau-tt^\dagger)\rangle$ signals the appearance of FP resonances between the barriers. With the change of variables, $\tau=\mathrm{sech}^2 x$, the new density, $\nu(x)$, has a finite value at $x=0$ whenever $\rho(\tau)$ has an inverse square-root singularity at $\tau=1$. It also proved useful to introduce the resolvent function, $G(z)$, defined as

$$G(z) \equiv \int_0^\infty dx \frac{\nu(x)}{z-\sinh^2 x}. \tag{65}$$

Both $\nu(x)$ and $G(z)$ can be obtained from the pseudocurrent $K(x)$ through the formulas

$$\nu(x) = \frac{2}{\pi}\mathrm{Im}\, K(x + i\pi/2 - i0^+) \tag{66}$$

and

$$G(z) = \frac{-K[\cosh^{-1}(\sqrt{-z})]}{\sqrt{z(1+z)}}, \tag{67}$$

respectively. Using Eqs. (66) and (67) together with Eqs. (63) and (64), the behavior of $\nu(x)$ and $G(z)$ for arbitrary values of T_1 and T_2 was studied in Ref. 23. The final results can be summarized by introducing the auxiliary variables $\zeta = T_2(1+T_1)/T_1$ and $\zeta_0=(1+T_1)/(1-T_1)$. There are five different regimes (see Fig. 1): (i) two gapped phases ($0<\zeta<1$ and $\zeta>\zeta_0$), (ii) two transition lines ($\zeta=1$ and $\zeta=\zeta_0$), and (iii) a gapless FP phase ($1<\zeta<\zeta a_0$). The density $\nu(x)$ exhibits the following behavior. For the gapless phase,

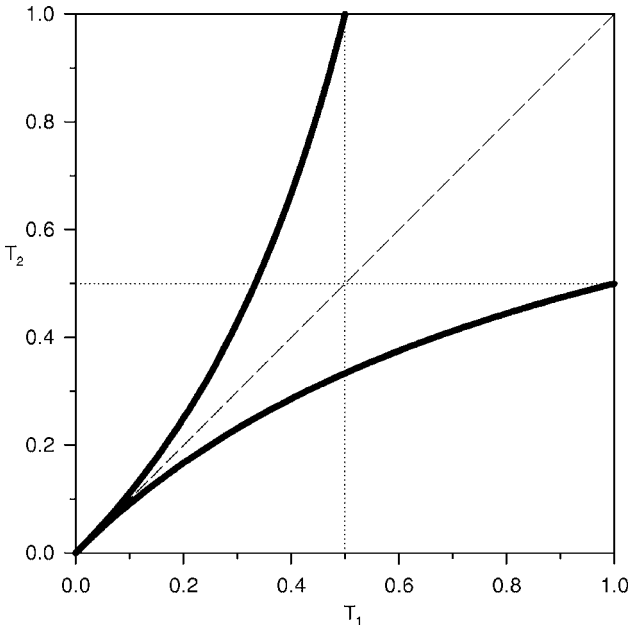

FIG. 1. Diagram illustrating the transport regimes as a function of the tunnel probabilities. The solid lines represent the transition lines $\zeta=\zeta_0$ and $\zeta=1$. The region above and below these solid lines are gapped phases, while the region in between is the gapless Fabry-Perot phase. The dashed line represents the particular case $T_1=T_2$, whereas the dotted lines are guides to the eye at $T_1=0.5$ and $T_2=0.5$.

$$\nu(x) \sim \nu(0), \quad x \to 0.$$

For the transition line,

$$\nu(x) \sim x^{1/3}, \quad x \to 0.$$

For the gapped phase,

$$\nu(x) = 0, \quad x < x_0.$$

Defining the reduced variable $t \equiv \zeta - \zeta_c$, where ζ_c denotes the position of a transition line ($\zeta_c=1$ or $\zeta_c=\zeta_0$), we may introduce "critical exponents" β, δ, and γ, through the relations: (i) $G(0)\sim|t|^{-\gamma}$ in the gapped phases, (ii) $\nu(x)\sim x^{1/\delta}$ at the transition lines, and (iii) $\nu(0)\sim|t|^\beta$ in the gapless phase. Interestingly, one finds $\beta=1/2$, $\delta=3$, and $\gamma=1$, which satisfies "Widom's scaling relation" $\gamma=\beta(\delta-1)$ with classical mean-field (saddle-point) values. The exact expression for $\nu(0)$ in the gapless FP phase is given by

$$\nu(0) = \frac{2N}{\pi}\frac{\sqrt{(T_1T_2)^2-(T_1-T_2)^2}}{T_1+T_2-T_1T_2}. \tag{68}$$

Although no formal proof was put forward in Ref. 23, strong evidence was presented for the classification of this quantum transition as a continuous phase transition.

V. DIFFERENTIAL CONDUCTANCE: ANOMALOUS POWER-LAW BEHAVIOR

In this section, we shall discuss the consequences of the continuous quantum transition described in Sec. IV to the

average differential conductance, Eq. (52), computed from the renormalization group flow equation. In order to make contact with the circuit theory equations, (63) and (64), we relate $\langle g(\varepsilon)\rangle$ to the pseudocurrent $K(x)$ as follows:

$$\langle g(\varepsilon)\rangle = \left.\frac{\varepsilon}{\sqrt{\varepsilon^2-1}}K(x)\right|_{\cosh x=\varepsilon}. \tag{69}$$

This equation will be thoroughly used in this section to obtain quantitative analytic prediction. We start by considering two limiting cases, where closed form solutions can be easily derived.

A. Quantum dot with symmetric barriers ($T_1=T=T_2$)

In this case, a closed form solution is possible because the fourth-degree polynomial equation, Eq. (63), factorizes into two quadratic equations and $K(x)$ becomes simply

$$K(x) = \frac{NT\sinh x}{2-T+T\cosh x}. \tag{70}$$

Inserting Eq. (70) into Eqs. (66) and (69), we find, respectively,

$$\nu(x) = \frac{2N}{\pi}\frac{T(2-T)\cosh x}{4(1-T)+T^2\cosh^2 x} \tag{71}$$

for the average density, and

$$\langle g(\varepsilon)\rangle = \frac{NT\varepsilon}{2+(\varepsilon-1)T} = \frac{NT\varepsilon}{2-T}+O(\varepsilon^2) \tag{72}$$

for the average conductance. Note that $\nu(0)=2NT/[(2-T)\pi]>0$ indicating the presence of FP resonances for all values of $0<T\leqslant 1$. As can be seen in Fig. 1, the line $T_1=T=T_2$ does not cross the transition lines $\zeta=1$ and $\zeta=\zeta_0$, thus confirming this prediction. For $\varepsilon\ll 1$, we may write the leading contribution as $\langle g(\varepsilon)\rangle=A\varepsilon^{\alpha}$, which implies $A=\pi\nu(0)/2$ and $\alpha=1$. This value for the exponent α is in agreement with the classification scheme put forward in Ref. 18.

Interestingly, with this symmetric barrier condition, the entire interaction effect can be absorbed into the barriers by renormalizing their transparencies as follows: $T(\varepsilon)=2\varepsilon T/[2+(\varepsilon-1)T]$ We remark that the same happens for the single barrier case, where no FP resonances exist. The renormalized barrier transparency then reads $T(\varepsilon)=\varepsilon^2T/[1+(\varepsilon^2-1)T]$. Note that in this case the exponent of $\langle g(\varepsilon)\rangle$ is $\alpha=2$.

B. Quantum dot with tunnel barriers ($T_1,T_2\ll 1$)

Here, a closed form, approximate solution is possible by neglecting terms proportional to T_1T_2 in the polynomial equation, which, similarly to the previous case, factorizes into two quadratic equations yielding

$$K(x) = \frac{NT_1T_2\sinh 2x}{2\sqrt{T_1^2+T_2^2+2T_1T_2\cosh 2x}}. \tag{73}$$

Inserting Eqs. (73) into Eq. (66), we find

$$\nu(x) = \frac{2NT_1T_2}{\pi(T_1+T_2)}\frac{\sinh x}{\sqrt{\tanh^2 x-\tanh^2 x_0}}, \tag{74}$$

where $\tanh x_0=|T_1-T_2|/(T_1+T_2)$. Computing the average conductance using Eq. (69), we get

$$\langle g(\varepsilon)\rangle = \frac{N\varepsilon^2T_1T_2}{\sqrt{(T_1-T_2)^2+4\varepsilon^2T_1T_2}}. \tag{75}$$

In this approximation, the transition lines merge into a single line $T_1=T_2$ and the order parameter, $\nu(0)$, develops a discontinuity, indicating that FP resonances appear as a first-order transition. Note that $\nu(0)=0, g(\varepsilon)\simeq N\varepsilon^2T_1T_2/|T_1-T_2|$ for $T_1\neq T_2$ and $\nu(0)=NT/\pi$, $g(\varepsilon)\simeq\pi\nu(0)\varepsilon/2$ for $T_1=T=T_2$. In this case too, renormalized tunnel barriers absorb completely the weak interaction effect. We find $T_1(\varepsilon)=[T_1-T_2+\sqrt{(T_1-T_2)^2+4\varepsilon^2T_1T_2}]/2$ and $T_2(\varepsilon)=[T_2-T_1+\sqrt{(T_1-T_2)^2+4\varepsilon^2T_1T_2}]/2$.

C. Quantum dot with two arbitrary barriers

We shall now discuss the general case of arbitrary T_1 and T_2. We consider again the auxiliary variables $\zeta=T_2(1+T_1)/T_1$ and $\zeta_0=(1+T_1)/(1-T_1)$. From Eq. (51), we note that the average conductance can be calculated directly from the average densities $\rho(\tau)$ or $\nu(x)$ using the formulas

$$g(\varepsilon) = \int_0^1 \frac{\varepsilon^2\tau\rho(\tau)d\tau}{1+(\varepsilon^2-1)\tau} = \int_0^{\infty}\frac{\varepsilon^2\nu(x)dx}{\varepsilon^2+\sinh^2(x)}. \tag{76}$$

Consequently, the behavior of $g(\varepsilon)$ in the limit $\varepsilon\to 0$ is determined by what happens to the density, $\nu(x)$, of the noninteracting system, in the vicinity of $x=0$, i.e., close to full transmission. As pointed out in Sec. IV B, reflectionless transmission can be attained in a double-barrier dot through the formation of Fabry-Perot resonances between the barriers, a pure wave-like phenomenon related to the phase-coherent motion of the electron in the dot. In fact, $\nu(0)$ can be interpreted as a measure of the density of these Fabry-Perot modes. By varying ζ at fixed ζ_0, one observes a suppression of $\nu(0)$ that ultimately leads to the onset of a quantum transition taking place both at $\zeta=1$ and $\zeta=\zeta_0$. One expects, therefore, a qualitative change in the behavior of $g(\varepsilon)$, for $\varepsilon\ll 1$, at these transition lines. The quantitative analysis presented below demonstrates that this is indeed what happens.

The low-energy behavior of the average conductance is generically given by a power law, $\langle g(\varepsilon)\rangle\simeq A\varepsilon^{\alpha}$, where the coefficient and the exponent depend strongly on which of the five regimes, described in Sec. III B, the system is in. A simple physical interpretation for the numerical value of the

exponent α can obtained by defining the average number of jumps for a complete charge transfer as $\bar{n}=2/\alpha$. For tunnel junctions, $\bar{n}=1$, indicating that the electron traverses the entire dot in a single leap, which is consistent with the notion that the dynamics inside the cavity is irrelevant in this case. For a symmetric dot, we find $\bar{n}=2$, implying a two-step process, i.e., the dominant mechanism of charge transfer is elastic resonant tunneling though Fabry-Perot states formed between the barriers. We present below the results for barriers with arbitrary transparencies.

(i) Gapped phase I ($0<\zeta<1$). In this regime, the average density, $\nu(x)$, exhibits a gap for $x \leqslant x_0$, where x_0 is a function of T_1 and T_2. We find

$$A_{gap}^{(1)} = \frac{NT_1T_2}{T_1 - T_2 - T_1T_2}, \quad \alpha_{gap} = 2. \tag{77}$$

(ii) Transition line I ($\zeta=1$). This regime is characterized by the power-law behavior, $\nu(x) \simeq (\sqrt{3}N/\pi)(T_1^2 x/2)^{1/3}$ for $x \to 0$, which yields

$$A_c^{(1)} = N\left(\frac{T_1^2}{2}\right)^{1/3}, \quad \alpha_c = 4/3. \tag{78}$$

(iii) Fabry-Perot phase ($1<\zeta<\zeta a_0$). In this regime, Fabry-Perot resonances acquire a finite density, $\sigma(0) = (2N/\pi)\sqrt{(T_1T_2)^2-(T_1-T_2)^2}/(T_1+T_2-T_1T_2)$, and we find

$$A_{FP} = \frac{\pi\nu(0)}{2}, \quad \alpha_{FP} = 1. \tag{79}$$

(iv) Transition line II ($\zeta=\zeta_0$). This is another transition line, and we get

$$A_c^{(2)} = N\left(\frac{T_2^2}{2}\right)^{1/3}, \quad \alpha_c = 4/3. \tag{80}$$

(v) Gapped phase II ($\zeta>\zeta_0$). This regime is similar to that of item (i) and, likewise, we find

$$A_{gap}^{(2)} = \frac{NT_1T_2}{T_2 - T_1 - T_1T_2}, \quad \alpha_{gap} = 2. \tag{81}$$

These regimes are illustrated in the diagram shown in Fig. 1, where cases (iv) and (ii) are represented as solid lines, while the regimes (v), (iii), and (i) correspond to the regions above, between, and below the solid lines, respectively. According to the classification scheme proposed in Ref. 18, in the gapped phases, cases (i) and (v), the exponent $\alpha_{gap}=2$ indicates that the dot behaves as a single barrier, since $\bar{n}_{gap}=1$. In the Fabry-Perot phase, case (iii), the exponent $\alpha_{FP}=1$ implies $\bar{n}_{FP}=2$, so that the electron jumps resonantly through the barriers in two steps. In the transition lines, cases (ii) and (iv), we have $\alpha_c=4/3$, which implies $\bar{n}_c=3/2=(\bar{n}_{gap}+\bar{n}_{FP})/2$. Physically, this means that the charge transfer process in this case is an evenly balanced statistical mixture of single and double jump events.

Finally, note that the vanishing of $\nu(0)$ as $\zeta \to 1^+$ and $\zeta \to \zeta_0^-$ is not sufficient to justify the appearance of the nonanalytic behavior $g(\varepsilon) \propto \varepsilon^{4/3}$ at $\zeta=1$ and $\zeta=\zeta_0$. A necessary condition, however, is a breakdown of the entire power expansion, i.e., a vanishing radius of convergence. This is precisely what happens. To show this, we consider the coefficient of the first analytic correction, which is proportional to A in regions (i) and (v). Observing that $A_{gap}^{(1)}=N\zeta(\zeta_0-1)/[2\zeta_0(1-\zeta)]$ and $A_{gap}^{(2)}=N\zeta(\zeta_0-1)/[2(\zeta-\zeta_0)]$ in regions (i) and (v), respectively, we conclude that the poles at $\zeta=1$ and $\zeta=\zeta_0$ indicate the breakdown of the power expansion. In Sec. VI, we shall propose an experimental procedure to measure the exponents α_{gap}, α_{FP}, and α_c.

VI. MEASURING THE EXPONENTS: UNIVERSAL FANO FACTOR

We believe that the results presented in Sec. V are amenable to experimental verification. A possible experiment might be a transport measurement on a double-barrier quantum dot defined on a two-dimensional electron gas (2DEG) of a high-mobility heterostructure. The first barrier might have a fixed transparency associated with the interface of an in-built junction. The second barrier, on the other hand, should be produced electrostatically by using a gate on top of the heterostructure. A negative voltage on the gate could be used to control the barrier's transparency and, therefore, the value of the variable ζ.[32] The experimental situation is similar to that of a second-order phase transition. Therefore, instead of addressing directly the "critical point," the experiment should be set to probe its vicinity. One possibility is to measure the prefactor A of the low-energy differential conductance $g(\varepsilon) \simeq A\varepsilon^{\alpha}$. In the vicinity of the transition line, we may define $t=\zeta-\zeta_c$, where $\zeta_c=1$ or $\zeta_c=\zeta_0$, and the theory predicts, for $N \gg 1$, the following behavior: $A \propto |t|^{1/2}$ in the FP phase and $A \propto |t|^{-1}$ in the adjacent gapped phase. Note that N plays the role of an extensive variable and thus one should take the "thermodynamic limit," $N \to \infty$. Finite N effects, such as tails in $\nu(x)$, however, are inevitable both experimentally and numerically, and should be dealt with by means of suitable techniques such as finite-size scaling.

The procedure above can be used to locate the transition line and measure the exponents α_{gap} and α_{FP}. The remaining exponent α_c can be obtained from a shot-noise measurement. The dimensionless shot-noise power is given by the renormalized Büttiker's formula

$$p(\varepsilon) = \sum_{n=1}^{N} \tau_n(\varepsilon)[1 - \tau_n(\varepsilon)]. \tag{82}$$

Its average value can be obtained from the RG flow equation (49) as follows:

$$\langle p(\varepsilon)\rangle = \frac{\varepsilon}{2}\frac{d}{d\varepsilon}\langle g(\varepsilon)\rangle. \tag{83}$$

In shot-noise measurements, one is usually concerned with the Fano factor, defined as $F(\varepsilon)=\langle p(\varepsilon)\rangle/\langle g(\varepsilon)\rangle$. At sufficiently low values of ε the Fano factor exhibits universal plateaus as a function of ζ for ζ_0 fixed. These plateaus correspond to the regions of the gapped and FP phases, so that $F(\varepsilon) \simeq \alpha_{gap}/2 \equiv F_{gap}=1/\bar{n}_{gap}$ for $0<\zeta<1$ and $\zeta>\zeta_0$ and $F(\varepsilon) \simeq \alpha_{FP}/2 \equiv F_{FP}=1/\bar{n}_{FP}$ for $1<\zeta<\zeta_0$. For small, but not

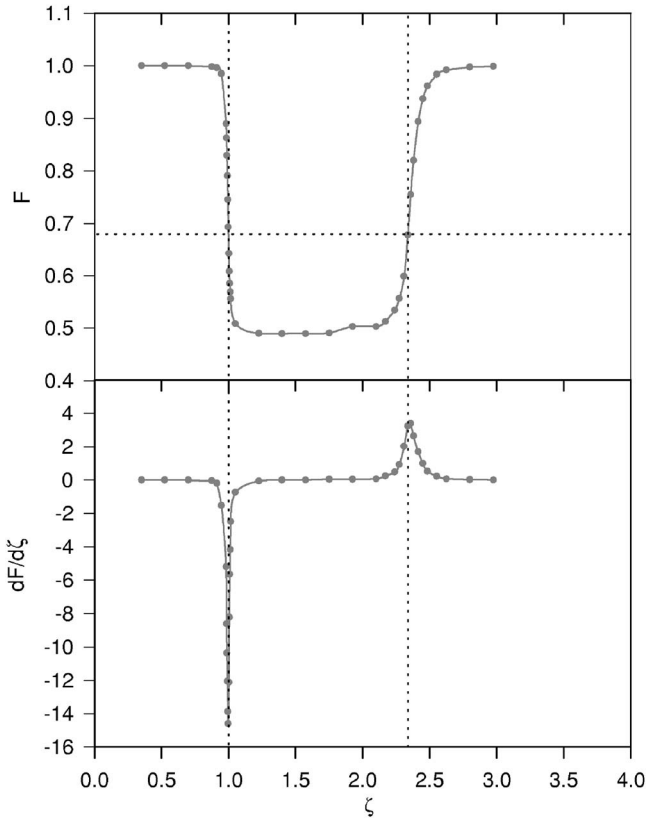

FIG. 2. Fano factor F and its derivative, $dF/d\zeta$, as a function of ζ for $T_1=0.4$. The dotted lines are numerical estimates for the transition lines, $\zeta=1$ and $\zeta=\zeta_0\simeq 2.33$, and for the critical value $F_c=\alpha_c/2\simeq 0.67$ for $\varepsilon\ll 1$.

vanishing values of ε, these plateaus are connected by a smooth crossover curve which intersects the transition lines $\zeta=1$ and $\zeta=\zeta_0$ at the value $F(\varepsilon)\simeq\alpha_c/2\equiv F_c=1/\bar{n}_c$. In Fig. 2, we illustrate this procedure by means of a numerical solution of the polynomial equation, Eq. (63). To check the consistency of the data, we located the transition lines from the extrema of $dF/d\zeta$ obtained from the numerical routine. The dotted lines indicate a graphical implementation of the procedure. Note that the theoretical prediction for $F(\varepsilon)$ at the transition lines coincides with the harmonic average of its values at the adjacent plateaus, i.e., $1/F_c=(1/F_{gap}+1/F_{FP})/2$, which follows from the relation $\bar{n}_c=(\bar{n}_{gap}+\bar{n}_{FP})/2$.

The universal values of the Fano factor at low voltages and low temperatures for weakly interacting quantum dots is another striking prediction of our model and, as we demonstrated above, should in principle be possible to observe experimentally.

VII. SUMMARY AND CONCLUSIONS

We studied the effects of weak Coulomb interactions in transport properties of quantum dots coupled via barriers of arbitrary transparencies to perfectly conducting leads. Using a combination of a renormalization group flow equation and and the supersymmetric nonlinear σ model, we demonstrated that a recently proposed extension of circuit theory provides an accurate description of the semiclassical regime of this system. Using this latter approach, we were able to predict the existence of an anomalous low-energy and low-temperature transport regime, which is a direct consequence of the onset of a continuous quantum transition associated to the formation of Fabry-Perot modes between the barriers. We also predicted a universal form for the Fano factor in the low-energy, low-temperature regime, which exhibits a sequence of plateaus as a function of the transparencies of the barriers. In the anomalous transport regime, the value of the Fano factor is the harmonic average of its values in adjacent plateaus.

Our approach to this problem has the potential to describe both perturbative quantum corrections such as weak-localization effects and nonperturbative effects, although much effort is still necessary to develop the appropriate tools. To be sure, the challenge to describe the nonperturbative aspects of quantum transport in open mesoscopic systems in the presence of Coulomb interactions, phase-coherence, dynamics, and chaotic dynamics is an enormous one. Nonetheless, from the recently reported progress, particularly in quantum dot systems, where the combination of field theoretical methods with random scattering matrix theory led to very useful constructive approaches,[6–8,10,12,13,31,33] there is ground for some optimism. In fact, from the combined results of these works it is possible to see that they provide essential and complementary ingredients for the construction of a tractable and very general dynamical theory of open interacting mesoscopic systems with chaotic dynamics.

Although the derivation of such a theory is currently beyond reach, it is possible to summarize its probable key elements. (i) Using the formulation put forward in Ref. 10, one should be able to derive the dynamical form of the boundary conditions obtained from elimination of the degrees of freedom inside the leads together with all macroscopic environment variables. The projection technique allows for a rigorous exploitation of time scale separations along with corresponding dissipative processes, thus bypassing the necessity to introduce unphysical, fictitious reservoirs in the description. (ii) The notion of nonlinear classical back actions from an electromagnetic environment discussed in Ref. 33 and related to the environmental formalism provides a clear understanding of the role of realistic detection schemes in the effective dynamics of the system and how they should be incorporated in the boundary conditions. (iii) The careful analysis of the structure of the saddle point presented in Ref. 12, separating pure phase fluctuations from changes in the distribution function, and the resulting form of the effective action with two coupled fields gives useful insight on how to deal with the inevitable nonlocality in time due to retardation effects. Whether the practical implementations of these concepts will lead to a constructive approach remains to be seen.

ACKNOWLEDGMENTS

This work was partially supported by CNPq, FACEPE, and FAP-SE (Brazilian Agencies).

[1] Y. Makhlin, G. Schön, and A. Shnirman, Phys. Rev. Lett. **85**, 4578 (2000); S. Pilgram and M. Büttiker, *ibid.* **89**, 200401 (2002).
[2] I. L. Aleiner, N. S. Wingreen, and Y. Meir, Phys. Rev. Lett. **79**, 3740 (1997); M. G. Vavilov and I. L. Aleiner, Phys. Rev. B **60**, R16311 (1999).
[3] I. L. Aleiner, P. W. Brouwer, and L. I. Glazman, Phys. Rep. **358**, 309 (2002).
[4] G. Murthy and H. Mathur, Phys. Rev. Lett. **89**, 126804 (2002).
[5] G. Murthy and R. Shankar, Phys. Rev. Lett. **90**, 066801 (2003).
[6] D. S. Golubev and A. D. Zaikin, Phys. Rev. B **69**, 075318 (2004).
[7] P. W. Brouwer, A. Lamacraft, and K. Flensberg, Phys. Rev. Lett. **94**, 136801 (2005).
[8] P. W. Brouwer, A. Lamacraft, and K. Flensberg, cond-mat/0502518 (unpublished).
[9] R. P. Feynman and F. L. Vernon, Ann. Phys. (N.Y.) **24**, 118 (1963).
[10] A. M. S. Macêdo, Phys. Rev. B **69**, 155309 (2004).
[11] K. B. Efetov, *Supersymmetry in Disorder and Chaos* (Cambridge University Press, Cambridge, 1997).
[12] A. Kamenev and A. Andreev, Phys. Rev. B **60**, 2218 (1999).
[13] D. B. Gutman, Y. Gefen, and A. D. Mirlin, in *Quantum Noise in Mesoscopic Systems*, edited by Yu. V. Nazarov (Kluwer Academic, Dordrecht, The Netherlands, 2003).
[14] H. Pothier, S. Guéron, N. O. Birge, D. Esteve, and M. H. Devoret, Phys. Rev. Lett. **79**, 3490 (1997).
[15] S. Nakajima, Prog. Theor. Phys. **20**, 948 (1958); R. Zwanzig, J. Chem. Phys. **33**, 1338 (1960); H. Mori, Prog. Theor. Phys. **33**, 423 (1965); B. Robertson, Phys. Rev. **144**, 151 (1966).
[16] For a review, see R. Balian, Y. Alhassid, and H. Reinhardt, Phys. Rep. **131**, 1 (1986).
[17] D. Boyanovsky and H. J. Vega, Ann. Phys. (N.Y.) **307**, 335 (2003).
[18] M. Kindermann and Yu. V. Nazarov, Phys. Rev. Lett. **91**, 136802 (2003).
[19] K. A. Matveev, D. Yue, and L. I. Glazman, Phys. Rev. Lett. **71**, 3351 (1993).
[20] M. H. Devoret, D. Esteve, H. Grabert, G.-L. Ingold, H. Pothier, and C. Urbina, Phys. Rev. Lett. **64**, 1824 (1990).
[21] A. M. S. Macêdo, Phys. Rev. B **66**, 033306 (2002).
[22] A. L. R. Barbosa and A. M. S. Macêdo, Phys. Rev. B **71**, 235307 (2005).
[23] A. M. S. Macêdo and A. M. C. Souza, Phys. Rev. E **71**, 066218 (2005).
[24] J. J. M. Verbaarschot, H. A. Weidenmüller, and M. R. Zirnbauer, Phys. Rep. **129**, 367 (1985).
[25] For a recent review, see L. S. Levitov, in *Quantum Noise in Mesoscopic Systems*, edited by Yu. V. Nazarov (Kluwer Academic, Dordrecht, The Netherlands, 2003).
[26] B. Rejaei, Phys. Rev. B **53**, R13235 (1996).
[27] M. Büttiker, H. Thomas, and A. Prêtre, Phys. Lett. A **180**, 364 (1993).
[28] G-L. Ingold and Yu. V. Nazarov, in *Single Charge Tunneling*, edited by H. Grabert and M. H. Devoret, NATO ASI Series B294 (Plenum, New York, 1992).
[29] C. L. Kane and M. P. A. Fisher, Phys. Rev. B **46**, 15233 (1992).
[30] D. A. Bagrets and Yu. V. Nazarov, cond-mat/0304339 (unpublished).
[31] P. W. Brouwer and C. W. J. Beenakker, J. Math. Phys. **37**, 4904 (1996).
[32] A similar setup has been constructed to observe reflectionless tunneling in NINIS junctions, see, e.g., H. Takayanagi, E. Toyoda, and T. Akazaki, Czech. J. Phys. **46**, 2507 (1996).
[33] M. Kindermann and Yu. V. Nazarov, in *Quantum Noise in Mesoscopic Systems*, edited by Yu. V. Nazarov (Kluwer Academic, Dordrecht, The Netherlands, 2003).